Analytical Biochemistry 388 (2009) 102–107

Contents lists available at ScienceDirect

Analytical Biochemistry

journal homepage: www.elsevier.com/locate/yabio

An aptamer-based biosensor for mammalian initiation factor eukaryotic initiation factor 4A

Akihiro Oguro [1], Takashi Ohtsu [2], Yoshikazu Nakamura *

Department of Basic Medical Sciences, Institute of Medical Science, University of Tokyo, Minato-ku, Tokyo 108-8639, Japan

ARTICLE INFO

Article history:
Received 7 December 2008
Available online 27 February 2009

Keywords:
Aptamer
eIF4A
Biosensor
SPR
Affinity purification

ABSTRACT

Aptamers are short single-stranded DNA or RNA sequences that are selected in vitro based on their high affinity to a target molecule. Here we demonstrate that an RNA aptamer selected against eukaryotic initiation factor 4A (eIF4A) serves as an efficient biosensor. The aptamer, when immobilized to resin, purifies eIF4A from crude cell extracts by affinity pull-down, and ^{32}P-labeled aptamer can detect some 300 ng of eIF4A by dot-blot analysis. Moreover, by use of an aptamer-immobilized sensor chip, we developed a surface plasmon resonance assay to detect eIF4A at the nanogram level within whole cell lysates after optimizing sample preparation, thereby showing a real-time sensor for eIF4A in cell extract solution.

The application of combinatorial technologies and molecular modeling for the discovery of synthetic ligands may open new avenues for the development of more efficient biosensor procedures to detect target proteins or molecules of interest. The concept of using single-stranded nucleic acids (aptamers) as affinity molecules for proteins was first described in 1990 [1,2]. The concept is based on the ability of short (20–80 mer) sequences to fold, in the presence of a target, into unique three-dimensional structures that bind the target with high affinity and specificity. Aptamers are generated by a process that combines combinatorial chemistry with in vitro evolution, known as SELEX[3] (systematic evolution of ligands by exponential enrichment), from a complex library of randomized sequences of typically 10^{14} different molecules [3–5]. Following the incubation of a protein with a library of DNA or RNA sequences, protein–RNA/DNA complexes are isolated, the sequence is amplified, and the process is repeated until the sample is enriched with sequences that display high affinity for the protein of interest. Recent advancements in RNA technology have greatly facilitated the discovery and development of aptamers for various application purposes such as affinity purification of proteins [6,7], biosensor for several biomarkers as well as diagnostics for therapeutic markers [8,9], and therapeutics for diseases [10]. The first aptamer-based therapeutic, pegaptanib (Macugen), targeting vascular endothelial growth factor, was approved by the U.S. Food and Drug Administration in December 2004 for the treatment of age-related macular degeneration (AMD) [11,12]. Considering the basic principle of aptamer selection, the high potential of RNA to create a vast set of tertiary structures is conceivable from both the "RNA world" hypothesis [13] and the concept of "molecular mimicry" between RNA and protein [14].

We previously isolated an RNA aptamer to eukaryotic initiation factor 4A (eIF4A) (referred to as 4Aapt [3]). eIF4A, together with eIF4E and eIF4G, are the subunits of the initiation factor complex eIF4F, which is required for the initial association of the small (40S) ribosomal subunit with messenger RNA (mRNA) [15,16]. (There are three known eIF4A gene products: eIF4AI, eIF4AII, and eIF4AIII; we focus on eIF4AI and refer to it as eIF4A throughout this text.) eIF4A is a prototype member of the DEAD box RNA helicase family that couples ATPase activity to RNA binding and unwinding [17–19]. Therefore, the apparent role of eIF4A is to facilitate the unwinding of the secondary structure present in the 5′ untranslated region of mRNAs that would otherwise impede translation initiation [20]. The isolated aptamer, 4Aapt, has a dissociation constant of 27 nM for eIF4A and severely inhibits ATP hydrolysis as well as cap-dependent in vitro translation [3].

Recently, a close relationship between aberrant expression of initiation factors and malignant transformation of mammalian cells has been described [21–25]. As for eIF4A, its elevated

* Corresponding author. Fax: +81 3 5449 5415.
E-mail address: nak@ims.u-tokyo.ac.jp (Y. Nakamura).
[1] Present address: Department of Molecular Biology, Jikei University School of Medicine, Minato-ku, Tokyo 105-8461, Japan.
[2] Present address: Division of Cancer Therapy, Kanagawa Cancer Center Research Institute, Asahi-ku, Kanagawa 241-0815, Japan.

[3] *Abbreviations used:* SELEX, systematic evolution of ligands by exponential enrichment; AMD, age-related macular degeneration; eIF4A, eukaryotic initiation factor 4A; 4Aapt, anti-eIF4A aptamer; mRNA, messenger RNA; SPR, surface plasmon resonance; PCR, polymerase chain reaction; DMEM, Dulbecco's modified Eagle's medium; FBS, fetal bovine serum; EDTA, ethylenediaminetetraacetic acid; BSA, bovine serum albumin; SDS–PAGE, sodium dodecyl sulfate–polyacrylamide gel electrophoresis; CBB, Coomassie Brilliant Blue; HRP, horseradish peroxidase; IgG, immunoglobulin G; PVDF, polyvinylidenefluoride; tRNA, transfer RNA; RU, resonance units; mTOR, mammalian target of rapamycin.

0003-2697/$ - see front matter © 2009 Elsevier Inc. All rights reserved.
doi:10.1016/j.ab.2009.01.046

expression is associated with melanomas [26] and a model of leukemia in mice [27]. Moreover, the tumor suppressor protein, Pdcd4, is shown to be a binding partner of eIF4A [28]. These findings emphasize the importance and utility of an efficient biosensor system for eIF4A as an alternative or equivalent to the antibody. For this purpose, this study aimed to use the 4Aapt as a tool for affinity purification, dot-blot detection, and surface plasmon resonance (SPR) sensor of eIF4A protein present in whole cell lysates.

Materials and methods

Protein and RNA preparations

Recombinant eIF4A protein was purified as either a His-tag fusion protein or a His-tag free protein produced by thrombin cleavage after purification, as described previously [3]. The 4Aapt sequence (referred to as RNA no. 20 in the previous article [3]), mutant 4Aapt sequence (referred to as M10 in the previous article [3]), and its control random (40 N) sequence were polymerase chain reaction (PCR) amplified from templates 5′-TAATACGACTCACTA TAGGGAGACAAGAATAAAACGCTCAAGGGGACCGCGCCCCACATGTGA GTGAGGCCGAAACGTAGATTCGACAGGAGGCTCACAACAGGC-3′, 5′-T AATACGACTCACTATAGGGAGACAAGAATAAAACGCTCAAGGGGACC GCGCCCCACATGAGAGGTAGGCCGAAACGTAGATTCGACAGGAGGCT CACAACAGGC-3′ (substituted nucleotides are underlined), and 5′-TAATACGACTCACTATAGGGAGACAAGAATAAAACGCTCAA(40 N)TTC GACAGGAGGCTCACA ACAGGC-3′, respectively, using a pair of forward (5′-TAATACGACTCACTATAGGGAGACAAGAATAAACGCTCAA-3′) and reverse (5′-GCCTGTTGTGAGCCTCCTGTCGAA-3′) primers (the T7 promoter sequence is underlined). To synthesize 3′ poly(A)-tailed 4Aapt or 40 N sequence, the reverse primer was substituted for by 5′-TTTTTTTTTTTTTTTTGCCTGTTGTGAGCCTCC TGTCGAA-3′. The PCR products were purified and used for in vitro transcription, and 4Aapt and N40 RNAs were prepared as described previously [3]. RNA transcripts used for dot-blot analysis were synthesized in the presence of [α-^{32}P]CTP (800 Ci/mmol) to a specific activity of 2×10^{17} cpm/mol RNA and prepared as above.

Preparation of crude cell extracts

HeLa and HEK293 cells were grown in Dulbecco's modified Eagle's medium (DMEM, Gibco) supplemented with 10% fetal bovine serum (FBS, Gibco), and CHP134 cells were grown in RPMI-1640 (Gibco) supplemented with 10% FBS, to 80 to 90% confluence in 100-mm cell culture dishes. Cultured cells were collected by centrifugation after trypsin treatment and were washed in phosphate-buffered saline to remove cell culture medium. HeLa cell extracts for pull-down and dot-blot assays were prepared by incubating cells (harvested from one culture dish) in 40 μl of buffer A (20 mM Tris–HCl [pH 7.6], 100 mM KCl, 2.5 mM magnesium acetate, and 1 mM ethylenediaminetetraacetic acid [EDTA]) supplemented with 0.01% NP40 and 5% protease inhibitor (1 tablet mini Complete [Roche] per 0.5 ml of buffer) on ice for 30 min, followed by centrifugation at 13,000*g* for 15 min. The resulting supernatants were used as cell extracts. To prepare cell extracts for SPR analysis, HeLa, HEK293, and CHP134 cells (harvested from one culture dish) were lysed in 100 μl of buffer A with 0.05% NP40, mixed with 40 μl of streptavidin–agarose (Sigma), and incubated at 4 °C for 30 min, followed by centrifugation. The supernatant was then mixed with 30 μl of a 10% slurry oligo(dT) type 7 cellulose (GE Healthcare, preequilibrated with buffer A and supplemented with 0.14 mg/ml bovine serum albumin [BSA] for masking the resin) and 10 μg of poly(A)-tailed random sequence RNA, incubated at 4 °C for 15 min, centrifuged, and subjected to the same treatment once again. Finally, the sample was passed through a 0.45-μm membrane filter (Millex-HV, syringe-driven filter unit, 4 mm diameter, Millipore). The total protein concentration was estimated by the Lowry method. RNase inhibitor (final concentration 1–2 U/μl, Takara) was added to the cell extracts before use.

RNA stability assay

After 10 μg of poly(A)-tailed 4Aapt RNA was mixed with 30 μl of a 10% slurry oligo(dT) type 7 cellulose (as described above), the resulting heteroduplex oligonucleotides were incubated with buffer A in the presence of 0.01% NP40 and 5% protease inhibitor or with the HeLa cell extract (as prepared above) at room temperature for 15 min in the presence of RNase inhibitor (final concentration 2 U/μl, Takara). After brief centrifugation, the resin was washed three times with 150 μl of buffer A and the 4Aapt was eluted by TE buffer and subjected to electrophoresis in 6% acrylamide/7 M urea/TBE gel. The 4Aapt RNA separated in the gel was detected and quantified by ethidium bromide staining.

Pull-down assay

The 4Aapt RNA (10 μg), mutant 4Aapt, or N40 random RNA was mixed with 10% slurry oligo(dT) beads (30 μl) and the HeLa cell extract (40 μl) and made to a final volume of 100 μl with buffer A. After 15 min of incubation at room temperature, the mixture was centrifuged at 2100*g* for 1 min and the resin was washed three times with 150 μl of buffer A containing 100, 150, 200, 250, or 300 mM KCl. Bound eIF4A protein was eluted with 30 μl of TE plus 0.5 μl of 10 mg/ml RNase A, mixed with sodium dodecyl sulfate–polyacrylamide gel electrophoresis (SDS–PAGE) sample buffer, and subjected to SDS–PAGE (8 or 10%), followed by staining with Coomassie Brilliant Blue (CBB), and analyzed by Western blotting using anti-eIF4AI polyclonal antibody (Santa Cruz Biotechnology) and anti-goat horseradish peroxidase (HRP)-conjugated immunoglobulin G (IgG, Santa Cruz Biotechnology) as described previously [3].

Dot-blot assay

Increasing amounts (0.01, 0.03, 0.1, 0.3, and 1 μg) of eIF4A and BSA proteins were spotted on polyvinylidenefluoride (PVDF) membrane (Immobilon-P, Millipore) that was presoaked with methanol for a few seconds and equilibrated with buffer B (20 mM Tris–HCl [pH 7.6], 100 mM potassium acetate, and 2.5 mM magnesium acetate) for 15 min at room temperature. The membrane was then soaked with buffer B containing 5% skim milk and 0.05% Tween 20 for 30 min at room temperature and washed with the same buffer B containing 0.05% Tween 20 for 15 min at room temperature two times. Then the spotted membrane was incubated with buffer B containing transfer RNA (tRNA, 0.2 mg/ml final concentration) and ^{32}P-labeled 4Aapt or N40 (random) RNA (2.5×10^5 cpm) for 2 h at 37 °C. Then the membrane washed with the buffer B containing 0.05% Tween 20 for 15 min at room temperature two times. The bound ^{32}P-labeled RNA was quantified using a BAS-2000 PhosphorImager (Fuji).

SPR assay

The SPR assays were performed essentially as described previously using the BIAcore 2000 instrument [29,30] according to the manufacturer's instructions. First, biotinylated-oligo(dT)$_{16}$ (0.02 mg/ml) was bound to the surface of streptavidin-coated sensor chip SA (GE Healthcare) at a flow rate of 20 μl/min in running buffer (20 mM Tris–HCl [pH 7.6], 100 mM KCl, 2.5 mM magnesium acetate, and 0.05% NP40). Then poly(A)-tailed 4Aapt and N40 RNAs were immobilized to the sensor chip by hybridization at a flow rate of 20 μl/min for 1 min. One uncoated flow cell was used for the ref-

erence. Sample solutions containing 0.1 mg/ml cell extracts and 1 mg/ml tRNA in the running buffer were injected into the flow cell, and the net interaction between RNA and protein was obtained by subtracting the blank flow cell data from the sample flow cell data.

Results and discussion

Aptamer-based affinity purification of eIF4A

The nonmodified 3′ end poly(A)-tailed 4Aapt RNA was immobilized to oligo(dT) beads and used as an affinity resin to purify eIF4A from crude cell extracts. The stability of nonmodified poly(A)-tailed 4Aapt RNA was first examined by denaturing PAGE after mixing the immobilized beads with HeLa cell extract for 15 min. As shown in Fig. 1, there was no appreciable degradation of the immobilized RNA (lane 2, arrow), although there appeared to be a small fraction of slightly degraded RNA (lane 2, arrowhead). In any case, the degradation appears to be limited to exonucleolytic degradation of a few nucleotides, and this is not expected to affect the affinity of 4Aapt given that it would remove only a small part of the 3′ poly(A) tail or the 5′ flanking region of 4Aapt. Neither is crucial for affinity [3]. Under these conditions, proteins associated with the 4Aapt affinity bead were pulled down and analyzed by SDS–PAGE and Western blotting using anti-eIF4A antibody (Fig. 2). At 100 mM KCl concentration, some proteins of distinct molecular masses coprecipitated with 4Aapt and also mutant 4Aapt that lost the affinity to eIF4A are shown on the CBB-stained gel, especially two major proteins around 45 kDa, molecular mass of eIF4A (Fig. 2A, lanes 1 and 6). These two bands coprecipitated with mutant 4Aapt steadily disappeared on increasing KCl concentrations to 150, 200, 250, and 300 mM (Fig. 2A, lanes 7–10), but one protein is still coprecipitated with 4Aapt at high KCl concentration (Fig. 2A, lanes 2–5, arrowhead). Western blot analysis revealed that this protein is reactive to anti-eIF4A antibody (Fig. 2B, lanes 7 and 8, arrowhead), and no such reactive protein is found in coprecipitants with control N40 random RNA (Fig. 2B, lanes 5 and 6). At lower KCl concentrations, eIF4A is likely to overlap with, or be hidden by, two nonspecific binding proteins around 45 kDa that are coprecipitable with 4Aapt and mutant 4Aapt (Fig. 2A, lanes 1 and 6). These nonspecific binding proteins that coprecipitated, but did not react, with anti-eIF4A antibody are detected with both N40 random RNA and mutant 4Aapt (data not shown). Although the other minor associated proteins remain to be clarified, these results clearly demonstrate that the 4Aapt-immobilized resin is able to affinity purify eIF4A from crude cell extracts.

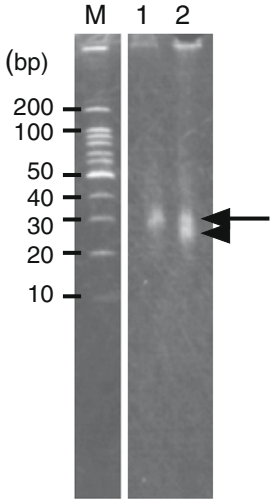

Fig. 1. RNA stability in crude cell extracts. Poly(A)-tailed 4Aapt RNA immobilized on the oligo(dT) type 7 cellulose was incubated with cell lysis buffer or HeLa cell extract, and the residual RNA was subjected to 6% denaturing PAGE, followed by staining with ethidium bromide. Experimental conditions and procedures are described in Materials and Methods. Lane M: size markers (dsDNA); lane 1: poly(A)-tailed 4Aapt RNA incubated with cell lysis buffer; lane 2: poly(A)-tailed 4Aapt RNA incubated with HeLa cell extract. The arrow indicates the full-length poly(A)-tailed 4Aapt, and the arrowhead indicates the slightly degraded RNA product.

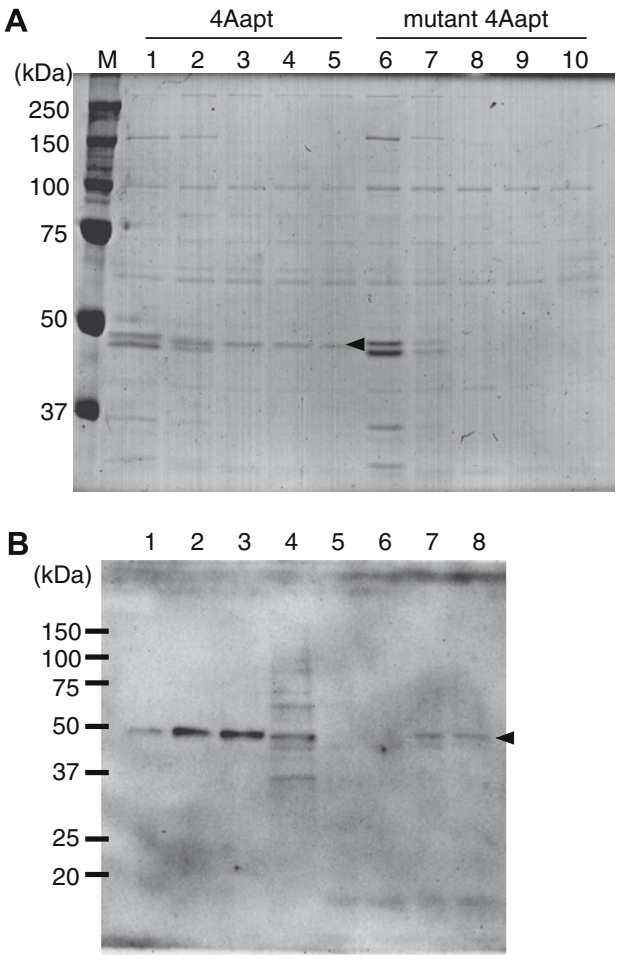

Fig. 2. Affinity purification of eIF4A from crude cell extracts by 4Aapt resin. The poly(A)-tailed 4Aapt RNA, mutant 4Aapt, or N40 random RNA immobilized to oligo(dT) beads was incubated with HeLa cell extract, and proteins coprecipitated were subjected to SDS–PAGE, followed by CBB staining (A) and Western blotting using anti-eIF4AI antibody (B). Experimental conditions and procedures are described in Materials and Methods. (A) Lane M: protein size markers; lanes 1 and 6: coprecipitate washed with 100 mM KCl; lanes 2 and 7: coprecipitate washed with 150 mM KCl; lanes 3 and 8: coprecipitate washed with 200 mM KCl; lanes 4 and 9: coprecipitate washed with 250 mM KCl; lanes 5 and 10: coprecipitate washed with 300 mM KCl. Lanes 1 to 5: precipitated with 4Aapt; lanes 6 to 10: precipitated with mutant 4Aapt that lost the affinity to eIF4A. (B) Lane 1: eIF4A (50 ng); lane 2: eIF4A (100 ng); lane 3: eIF4A (200 ng); lane 4: HeLa cell extract (0.5 μl); lane 5: coprecipitate with N40 random RNA washed with 100 mM KCl; lane 6: coprecipitate with N40 random RNA washed with 200 mM KCl; lane 7: coprecipitate with 4Aapt washed with 100 mM KCl; lane 8: coprecipitate with 4Aapt washed with 200 mM KCl.

Dot-blot monitoring of eIF4A with aptamer probe

^{32}P-labeled 4Aapt RNA was also used as a probe for sensing eIF4A protein when blotted or spotted to PVDF membrane. eIF4A separated by SDS–PAGE was blotted to PVDF membrane, renatured by a process similar to that for far-Western analysis, and then incubated with ^{32}P-labeled 4Aapt. However, no ^{32}P signal appeared by

autoradiography (data not shown). Unlike the antibody, the 4Aapt is known to recognize a large area of the eIF4A protein, spanning the C- and N-terminal domains, and recognition of both of these domains is a prerequisite for high affinity [3]. Therefore, the above observation can be interpreted to indicate that eIF4A could not be fully renatured on the membrane and, therefore, is not a binding substrate to the aptamer. In contrast, the ^{32}P-labeled 4Aapt is able to detect native eIF4A from a minimum of 300 ng (Fig. 3, middle), spotted on the membrane, whereas no false-positive signal was observed between ^{32}P-labeled 4Aapt and BSA or between ^{32}P-labeled N40 random RNA and eIF4A (Fig. 3, upper and lower).

Use of 4Aapt with SPR to detect eIF4A in whole cell lysates

A real-time (semi)quantitative system to monitor, without the use of labeled probes, eIF4A in whole cell lysates will be of basic and applied importance due to the close relationship between the cellular level of eIF4A and tumorigenesis [26,27]. The SPR assay provides such a system through the use of a 4Aapt-immobilized sensor chip. To our knowledge, there is no report that used BIAcore instruments to directly analyze whole cell lysates. To this aim, we optimized the conditions to prepare crude cell extracts prior to SPR analysis. Nonspecific binding components were removed by passaging the cell extract against streptavidin beads and poly(A)-tailed N40 (random)/oligo(dT) beads. This was followed by passing the cell lysate through a 0.45-μM membrane to remove cell debris or other aggregates (see Materials and Methods). The resulting HeLa cell extract (2 μg of total protein) was injected into the flow cell in the presence of tRNA. As shown in Fig. 4, the resonance units (RU) increased to approximately 150 RU on the aptamer chip, whereas the same extract yielded 40 to 50 RU on the N40 (control) chip, thereby showing a net increase of 100 to 110 RU.

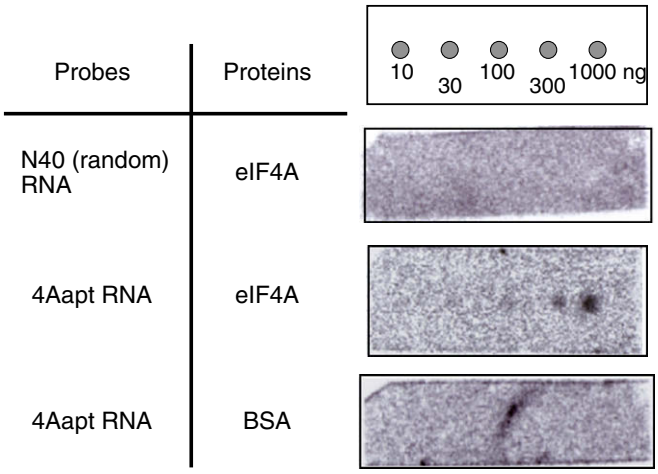

Fig. 3. Dot-blot analysis with the aptamer probe. Here 10, 30, 100, 300, and 1000 ng of eIF4A (upper and middle) or BSA (lower) were spotted on PVDF membrane and incubated with the indicated ^{32}P-labeled 4Aapt and N40 (random) RNAs. The reactivities of ^{32}P-labeled 4A aptamer probes to eIF4A and BSA spotted membranes are shown in the middle and lower panels, respectively. Experimental conditions and procedures are described in Materials and methods.

To estimate the amount of eIF4A that corresponds to this RU value, cell extracts containing exogenous eIF4A at 10, 30, and 100 ng were analyzed. The data indicate that 10, 30, and 100 ng of eIF4A gave rise to 50, 120, and 210 net RU, respectively, over the level achieved by cell extract alone (Fig. 4). Therefore, 100 to 110 RU can be estimated at approximately 35 ng of eIF4A, suggesting that 1 μg of total protein of HeLa cell extract contains approximately 17.5 ng of eIF4A according to the SPR measurement. This value turns out to be slightly larger than that estimated by Western blotting using anti-eIF4A antibody. Referring to the standard intensity of pure eIF4A protein bands, the amount of eIF4A present in 1 μg of total protein of HeLa extract is estimated to be 5 to 10 ng (Fig. 5A). This value is at nearly the same level as that in the previous report by Duncan and Hershey [31]. We estimate that the slight overestimation of eIF4A in cell extracts by SPR assay might be due to the presence of other binding components to eIF4A or masking agents in the crude cell extract. Nevertheless, these findings demonstrate that the aptamer chip is sensitive to detect in real time at least 10 ng of eIF4A present in the whole cell lysate by SPR.

Sensitivity of 4Aapt-based SPR assay to detect different cellular levels of eIF4A

We then asked whether the SPR assay could discriminate the difference between endogenous eIF4A levels in different cell lines. To this end, the endogenous amount of eIF4A was first monitored in cell lysates of HeLa, CHP134, and HEK293 cell lysates by Western blotting with the anti-eIF4A antibody. As shown in Fig. 5B, the relative abundance of eIF4A was shown to be in the order of HEK293 > HeLa > CHP134. With this reference, each extract (2 μg of total protein) was then injected into the SPR flow cell. As shown in Fig. 6, the level of RU increases to the same order estimated by Western blotting. Based on the previous estimate of endogenous eIF4A in HeLa extracts (i.e., 35 ng per injected microgram [μg] of protein cell extract), it is estimated that CHP134 and HEK293 con-

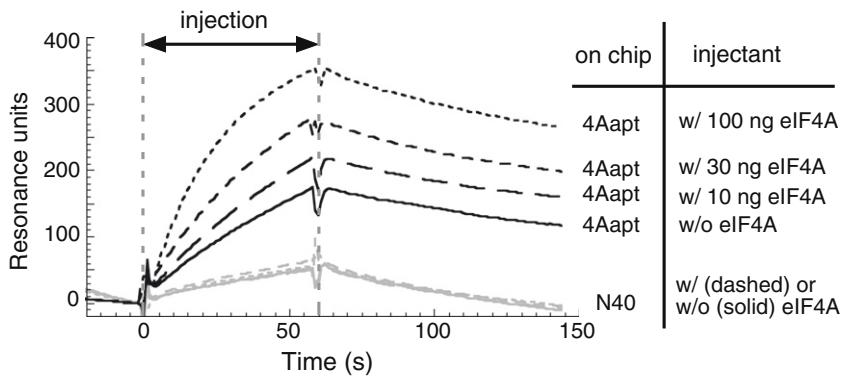

Fig. 4. SPR sensorgrams. 3′-Poly(A)-tailed 4Aapt and N40 (random) RNAs were immobilized to the streptavidin sensor chip via hybridization to a 5′-biotinylated oligo(dT), and the chip was injected with HeLa cell extracts (2 μg) containing the indicated exogenous eIF4A. Experimental conditions and procedures are described in Materials and Methods. w/, with; w/o, without.

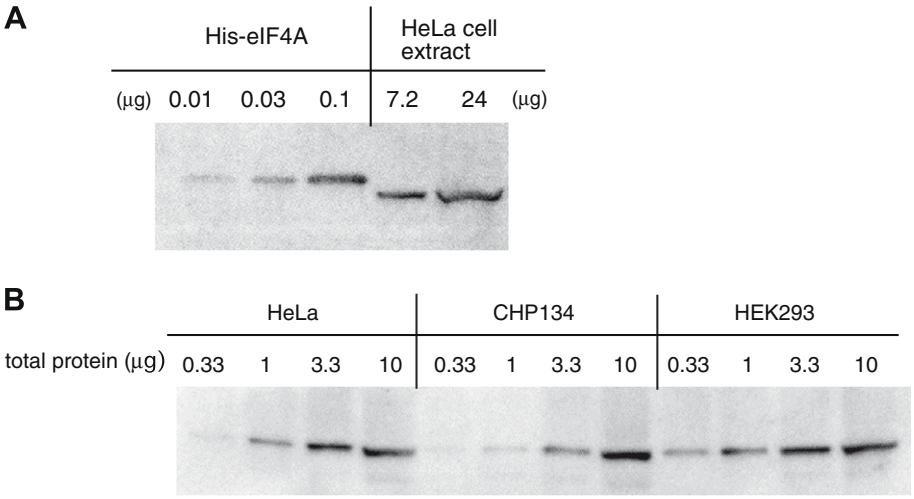

Fig. 5. Western blotting. (A) The indicated eIF4A samples (the His-tagged form has a slightly increased molecular mass) and HeLa cell extracts were subjected to SDS–PAGE and analyzed by Western blotting using anti-eIF4A antibody as described in Materials and Methods. (B) The abundance of endogenous eIF4A in three different cell lines was analyzed by Western blotting using anti-eIF4A antibody. The indicated amounts of extracts were subjected to SDS–PAGE.

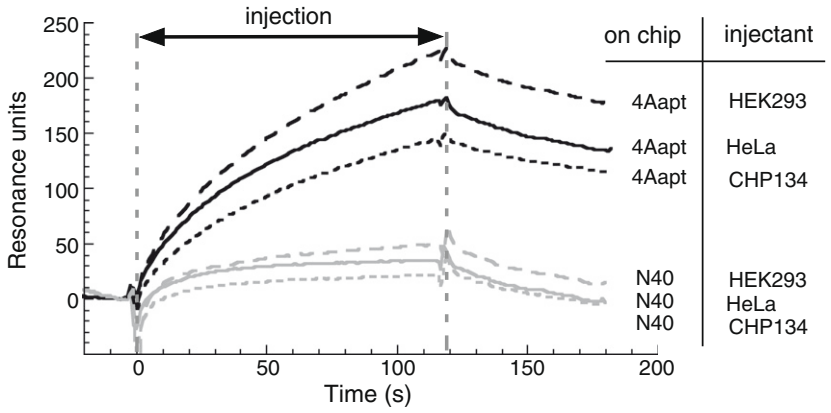

Fig. 6. SPR measurement of eIF4A present in crude extracts from different cell lines. Sensorgrams show the interaction between 4Aapt and eIF4A in cell extracts from HeLa, HEK293, and CHP134 cells. Here 2 μg of each cell extract was injected into the flow cells containing either the 4Aapt chip (black lines) or the N40 chip (gray lines).

tain approximately 20 and 57 ng of eIF4A, respectively, per injected μg of protein cell extract.

Conclusions

In this study, we developed the detection system of eIF4A from cell extract solution using the SPR sensor chip immobilizing anti-eIF4A RNA aptamer. With this system, we could detect eIF4A at the nanogram level within whole cell lysates after optimizing sample preparation. Although the causal relationship between tumor progression and overexpression of eIF4A remains to be studied, aberrant expression of eIF4A is associated with some human melanoma cells [26] and a leukemia model in mice [27]. Moreover, Pdcd4, previously identified as a tumor suppressor protein, turns out to be a binding partner of eIF4A [28]. Reexpression of Pdcd4 in cancer cells induces apoptosis and inhibits tumor growth. Furthermore, Pdcd4 is rapidly degraded on phosphorylation by the mTOR (mammalian target of rapamycin)-signaling pathway [32]. Considering these findings, the SPR assay system developed in this work provides a rapid, (semi)quantitative, label-free system to directly assay eIF4A in several cell lines, including clinical isolates. The recent development of an RNA microarray-based SPR system [33] will also greatly facilitate the utility of the SPR assay to screen whole cell lysates using existing RNA aptamers as well as new ones.

Acknowledgments

We thank Katsushi Koda and Eiko Takada for technical support, and we thank Colin Crist for critical reading of the manuscript and valuable suggestions. This work was supported in part by grants from the Ministry of Education, Sports, Culture, Science, and Technology of Japan (MEXT) and the Program for Promotion of Fundamental Studies in Health Sciences of the National Institute of Biomedical Innovation (NIBIO) as well as a Core Research for Evolution Science and Technology (CREST) grant from the Japan Science and Technology Agency.

References

[1] A.D. Ellington, J.W. Szostak, In vitro selection of RNA molecules that bind specific ligands, Nature 346 (1990) 818–822.
[2] C. Tuerk, L. Gold, Systematic evolution of ligands by exponential enrichment: RNA ligands to bacteriophage T4 DNA polymerase, Science 249 (1990) 505–510.
[3] A. Oguro, T. Ohtsu, Y.V. Svitkin, N. Sonenberg, Y. Nakamura, RNA aptamers to initiation factor 4A helicase hinder cap-dependent translation by blocking ATP hydrolysis, RNA 9 (2003) 394–407.
[4] S. Miyakawa, A. Oguro, T. Ohtsu, H. Imataka, N. Sonenberg, Y. Nakamura, RNA aptamers to mammalian initiation factor 4G inhibit cap-dependent translation by blocking the formation of initiation factor complexes, RNA 12 (2006) 1825–1834.
[5] S.P. Ohuchi, T. Ohtsu, Y. Nakamura, Selection of RNA aptamers against recombinant transforming growth factor-β type III receptor displayed on cell surface, Biochimie 88 (2006) 897–904.

[6] T.S. Romig, C. Bell, D.W. Drolet, Aptamer affinity chromatography: combinatorial chemistry applied to protein purification, J. Chromatogr. B 731 (1999) 275–284.
[7] M. Blank, T. Weinschenk, M. Priemer, H. Schluesener, Systematic evolution of a DNA aptamer binding to rat brain tumor microvessels, J. Biol. Chem. 276 (2001) 16464–16468.
[8] S. Tombelli, M. Minunni, M. Mascini, Aptamers-based assays for diagnostics, environmental, and food analysis, Biomol. Eng. 24 (2007) 191–200.
[9] R. Stoltenburg, C. Reinemann, B. Strehlitz, SELEX: A (r)evolutionary method to generate high-affinity nucleic acid ligands, Biomol. Eng. 24 (2007) 381–403.
[10] S.M. Nimjee, C.P. Rusconi, B.A. Sullenger, Aptamers: An emerging class of therapeutics, Annu. Rev. Med. 56 (2005) 555–583.
[11] E.W. Ng, D.T. Shima, P. Calias, E.T. Cunningham Jr., D.R. Guyer, A.P. Adamis, Pegaptanib a targeted anti-VEGF aptamer for ocular vascular disease, Nat. Rev. Drug Discov. 5 (2006) 123–132.
[12] B. Zhou, B. Wang, Pegaptanib for the treatment of age-related macular degeneration, Exp. Eye Res. 83 (2006) 615–619.
[13] R.F. Gesteland, T.R. Cech, J.F. Atkins, The RNA World, Cold Spring Harbor Laboratory Press, Cold Spring Harbor, NY, 1999.
[14] Y. Nakamura, Molecular mimicry between protein and tRNA, J. Mol. Evol. 53 (2001) 282–289.
[15] A-C. Gingras, B. Raucht, N. Sonenberg, EIF4 initiation factors: Effectors of mRNA recruitment to ribosomes and regulators of translation, Annu. Rev. Biochem. 68 (1999) 913–963.
[16] J.W.B. Hershey, W.C. Merrick, Pathway and mechanism of initiation of protein synthesis, in: N. Sonenberg, J.W.B. Hershey, M.B. Mathews (Eds.), Translational Control of Gene Expression, Cold Spring Harbor Laboratory Press, Cold Spring Harbor, NY, 2000, pp. 33–88.
[17] J. Yoder-Hill, A. Pause, N. Sonenberg, W.C. Merrick, The p46 subunit of eukaryotic initiation factor (eIF)-4F exchanges with eIF-4A, J. Biol. Chem. 268 (1993) 5566–5573.
[18] A. Pause, N. Sonenberg, Helicases and RNA unwinding in translation, Curr. Opin. Struct. Biol. 3 (1993) 953–959.
[19] F. Rozen, I. Edery, K. Meerovitch, T.E. Dever, W.C. Merrick, N. Sonenberg, Bidirectional RNA helicase activity of eukaryotic translation initiation factors 4A and 4F, Mol. Cell. Biol. 10 (1990) 1134–1144.
[20] N. Sonenberg, MRNA 5 cap-binding protein eIF4E and control of cell growth, in: J.W.B. Hershey, M.B. Mathew, N. Sonenberg (Eds.), Translational Control, Cold Spring Harbor Laboratory Press, Cold Spring Harbor, NY, 1996, pp. 245–269.
[21] A. Lazaris-Karatzas, K.S. Montine, N. Sonenberg, Malignant transformation by a eukaryotic initiation factor subunit that binds to mRNA 5 cap, Nature 345 (1990) 544–547.
[22] T. Fukuchi-Shimogori, I. Ishii, K. Kashiwagi, H. Mashiba, H. Ekimoto, K. Igarashi, Malignant transformation by overproduction of translation initiation factor eIF4G malignant transformation by overproduction of translation initiation factor eIF4G, Cancer Res. 57 (1997) 5041–5044.
[23] N. Brass, D. Heckle, U. Sahin, M. Pfreundschuh, G.W. Sybrecht, E. Meese, Translation initiation factor eIF4γ is encoded by an amplified gene and induces an immune response in squamous cell lung carcinoma, Hum. Mol. Genet. 6 (1997) 33–39.
[24] A.D. Benedetti, A.L. Harris, EIF4E expression in tumors: Its possible role in progression of malignancies, Intl. J. Biochem. Cell Biol. 31 (1999) 59–72.
[25] L. Zhang, X. Pan, J.W.B. Hershey, Individual overexpression of five subunits of human translation initiation factor eIF3 promotes malignant transformation of immortal fibroblast cells, J. Biol. Chem. 282 (2007) 5790–5800.
[26] J. Eberle, K. Krasagakis, C.E. Orfanos, Translation initiation factor eIF-4A1 mRNA is consistently overexpressed in human melanoma cells in vitro, Intl. J. Cancer 71 (1997) 396–401.
[27] Y-W. Lin, A.D. Aplan, Gene expression profiling of precursor T-cell lymphoblastic leukemia/lymphoma identifies oncogenic pathways that are potential therapeutic targets, Leukemia 21 (2007) 1276–1284.
[28] H.S. Yang, M.H. Cho, H. Zakowicz, G. Hegamyer, N. Sonenberg, N.H. Colburn, A novel function of the MA-3 domains in transformation and translation suppressor Pdcd4 is essential for its binding to eukaryotic translation initiation factor 4A, Mol. Cell. Biol. 24 (2004) 3894–3906.
[29] T. Mori, A. Oguro, T. Ohtsu, Y. Nakamura, RNA aptamers selected against the receptor activator of NFκ-B acquire general affinity to proteins of the tumor necrosis factor receptor family, Nucleic Acids Res. 32 (2004) 6120–6128.
[30] K. Mochizuki, A. Oguro, T. Ohtsu, N. Sonenberg, Y. Nakamura, High affinity RNA for mammalian initiation factor 4E interferes with mRNA-cap binding and inhibits translation, RNA 11 (2005) 77–89.
[31] R. Duncan, J.W.B. Hershey, Identification and quantification of levels of protein synthesis initiation factors in crude HeLa cell lysates by two-dimensional polyacrylamide gel electrophoresis, J. Biol. Chem. 258 (1983) 7228–7235.
[32] N.V. Dorrello, A. Peschiaroli, D. Guardavaccaro, N.H. Colburn, N.E. Sherman, M. Pagano, S6K- and -TRCP-mediated degradation of PDCD4 promotes protein interaction and cell growth, Science 314 (2006) 467–471.
[33] Y. Li, H.J. Lee, R.M. Corn, Fabrication and characterization of RNA aptamer microarrays for the study of protein–aptamer interactions with SPR imaging, Nucleic Acids Res. 34 (2006) 6416–6424.